Sheet Plasma Excitation by a 2.45 GHz Microwave Power Introduced through a Local Gas Injection Type Dielectric Window

Arnold Rey B. GINES and Motoi WADA

Graduate School of Science and Engineering, Doshisha University, Kyotanabe, Kyoto 610-0394, Japan

A 2.45 GHz microwave power injected through a quartz glass window produced a stable sheet-shaped plasma with the 11 cm wide and 4 cm high rectangular cross section in a static linear magnetic field. A thin slot gas conduit opened near the surface of the window supplied a discharge gas forming a stream of neutral atoms that intersected perpendicularly the plasma flowing toward the window along the magnetic field. The gas stream caused the change of the luminous intensity distribution of the plasma around the microwave window indicating reduction of the local plasma heat load. The window did not show any damage for a continuous operation of plasma up to 2 kW microwave input power.

1. Introduction

Effects due to change in magnetic field intensity to sustain plasmas have been discussed by several researchers [1–6]. Krinberg [1] observed the limit whereby the effect of the applied magnetic field can be used to reduce the size of the plasma column, increase the electron temperature and the average ion charge. Hashemi *et al.* [2] reported that a constriction of the plasma flow was observed with a decrease in plasma jet radius causing an additional Joule heating in a plasma. Woo *et al.* [5] identified the effect of ion temperature anisotropy associated with the induction of a magnetic field.

A system was designed and has previously been reported in detail in [6] to produce stable sheet-shaped plasma with high density and temperature gradient to be utilized for surface processing application. It was shown that the production of localized electron cyclotron resonance (ECR) region effectively reduced the ignition power and increased the pressure range of stable plasma operation under 1 kW of microwave input power (P_{mw}). This report highlights the performance of the microwave plasma induction structure that should withstand a high-power density heat loading from the produced plasma. The present report on the system includes the transition from sub-ECR to creating a local ECR interaction region. Plasma conditions at the location distant from the plasma production region were measured and analyzed by data obtained from Langmuir probe measurements with optical luminous intensity distributions to observe sensitivity to magnetic field variation. The observation was performed in the region of minimum magnetic flux density, B, in the axial direction of the magnetized plasma. Such observation of plasma in

a similar field configuration was performed by Tarvainen *et al.* [7] who found increasing periodic instabilities with increasing magnetic field strength. There are several modifications from the original system: a local magnetic field structure produced by combination of a linear magnetic field and permanent magnets, and neutral gas flow injected to cover the vacuum side surface of the microwave window.

2. Experimental Setup

The main part of the locally magnetized ECR sheet plasma device is depicted in Fig. 1. The main chamber is composed of a stainless steel six-way crosses flange that is 33 cm long and 15 cm in diameter. A dry scroll pump coupled to a 260 ℓ/s turbomolecular pump evacuates the chamber down to $< 5 \times 10^{-5}$ Pa.
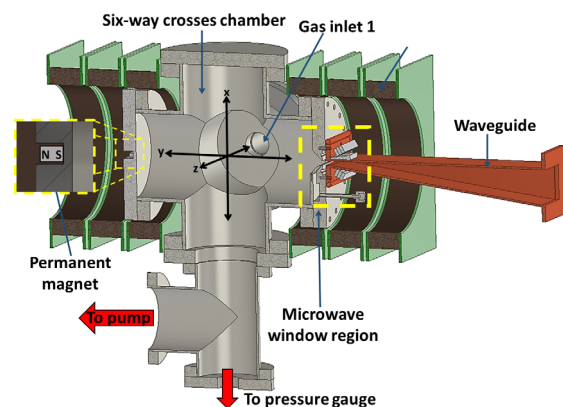
A detailed schematic of the microwave window re-

Fig. 1 Schematic diagram of the sheet plasma device.

author's e-mail: arnoldgines@gmail.com

gion is shown in Fig. 2. A 2.45 GHz microwave source can supply up to 3 kW of input power delivered by a tapered copper waveguide through a 7 mm by 110 mm window. A 5 mm thick quartz glass seals the vacuum while transmitting microwave power exposed to the plasma. The window maintains vacuum with a high temperature rubber O-ring, while a silicon rubber framed in copper sheet protects the quartz glass from any damage when in contact with the water-cooled waveguide flange. The water-cooled waveguide flange is attached to the main flange of the plasma chamber to reduce the local heating around the plasma excitation region.

A 1.5 mm by 110 mm slit shape gas conduit directs discharge gas to the vacuum side of the quartz glass to assist further cooling of the cathode region. In Fig. 2, red arrows, generated using Flowsquare 4.0 software, illustrate the flow of gas from the gas inlet to the planar slit and exiting towards the quartz window surface where a localized high pressure is created by the stream of gas. Continuous stable operation was achieved up to 2 kW P_{mw} for at least one hour without overheating the device. There is also another gas inlet port installed to feed the discharge gas into the central region of the plasma chamber. The location is indicated in Fig. 1 as gas inlet 1, and was used to confirm by comparison the effect of the local gas supply system of the planar slit.

A set of pancake coils made of wound copper wires and powered by a dc power supply are installed around the chamber to produce a linear magnetic field inside. When combined with the Nd-Fe permanent magnets installed in the microwave inlet region, a local electron cyclotron resonance (ECR) region is generated at the plasma down-

stream, a few mm from the plasma-facing quartz window surface. Another set of weaker permanent magnets is installed in the terminal wall, opposite flange to the microwave window, to enhance the expansion of the sheet plasma across the entire drift axis. Magnetic field lines along the microwave window region in Fig. 2 are generated using Metamesh 4.0 as illustrated by the brown broken line arrows. Figure 3 a) shows B inside the vacuum chamber induced by adjusting the current input in the pancake coils up to 15 A. The figure shows the field intensity distribution as a function of position y, measured from the center of the plasma chamber. On the plasma-facing surface of the quartz inlet window, the field is maximum and steeply decreases down to 200 G range along the central axis of the chamber at $y = 0$. The ECR condition is achieved starting at 14 A coil current. The B at this position is shown in Fig. 3 b) for varying coil current.

Images of the discharge showing the plasma thickness were captured using a Pentax K-7 digital camera and processed using ImageJ software, as shown in Fig. 4. The image is converted to an 8-bit grayscale file, as in Fig. 4 a), which linearly scales the image pixels to a 0 to 255 scale representing the image contrast based on pixel brightness and plotted for each row to create a 2-D plot of the intensity profile in Fig. 4 b).

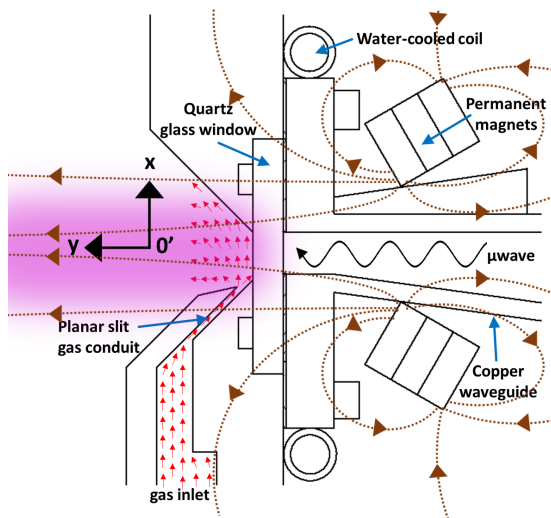Measurements of the electron temperature (T_e),

Fig. 2 Detailed schematic of the microwave window region. The red arrows represent direction of gas flow while the brown arrows with broken lines show the magnetic field emanating predominantly from the permanent magnets. 0' is at (0 mm, −16 mm, 0 mm) position.
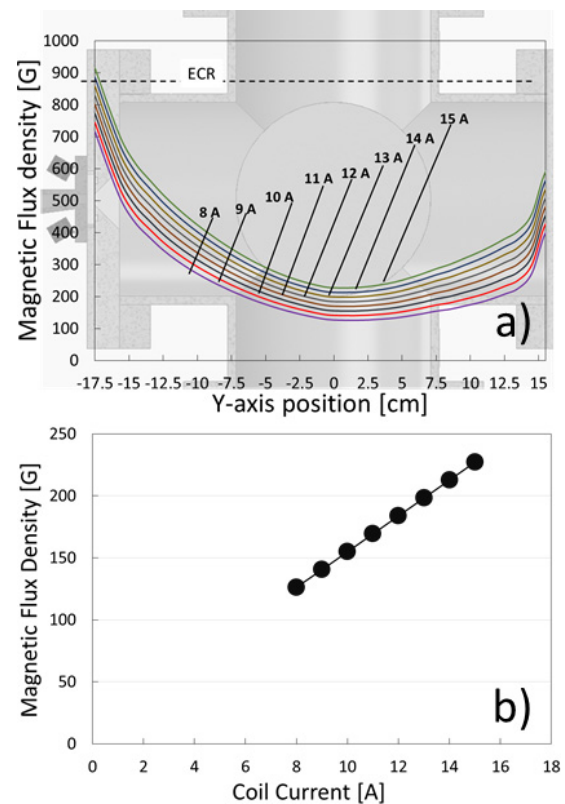

Fig. 3 (color online) Magnetic flux density profile inside the vacuum chamber at varying coil current a) along the central drift axis and b) at $y = -17.5$ cm position.
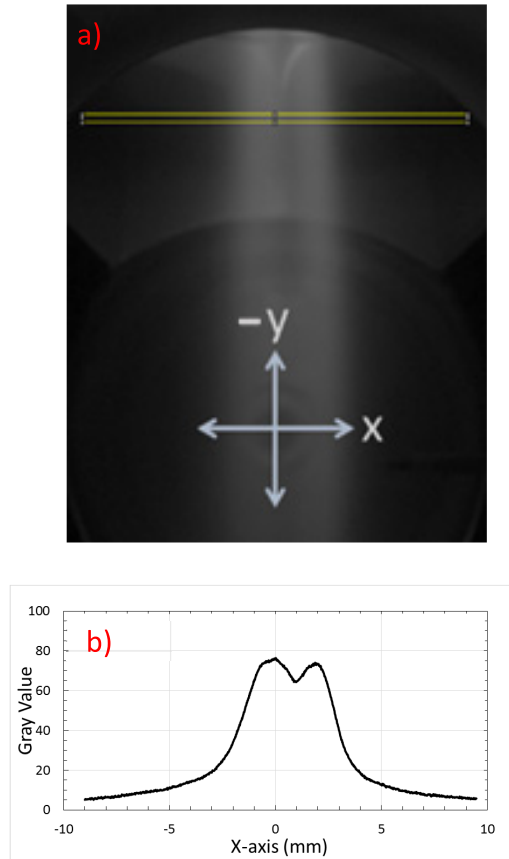
Fig. 4   Image processing of the plasma glow showing the a) actual image in 8-bit with the highlighted region of interest, b) plotted intensity values versus the relative position.

plasma density (n_e), plasma potential (V_{Plasma}) and floating potential (V_F) were carried out by using a 2 mm long cylindrical Langmuir probe of 0.6 mm diameter which can be moved vertically across the plasma sheet at $y = 0$. *I-V* characteristics were recorded for varying microwave input power and magnetic flux density.

3. Results

3.1   Plasma optical glow

Plots showing the Ar plasmas optical glow intensity versus the position at *x*-axis (direction of the sheet thickness) set perpendicular to the *y*-axis and the chamber axis for varying microwave power are shown in Fig. 5 for different intensities of the magnetic field. The intensity of the optical glow shows that the luminous intensity decreases towards higher magnetic field. At 0.5 kW, the optical glow appears to be more dispersed along the sheet thickness while also exhibiting the highest intensities of the plasma glow. The increased input power reduced the intensity of the plasma glow down to less than half the low power intensity at 2 kW. The observed sheet thickness which is estimated to be around 4 cm except at 0.5 kW agrees with the initial calculation of the plasma thickness from Larmor radius presented in [6]. From 1 kW, the assumed sheet thick-
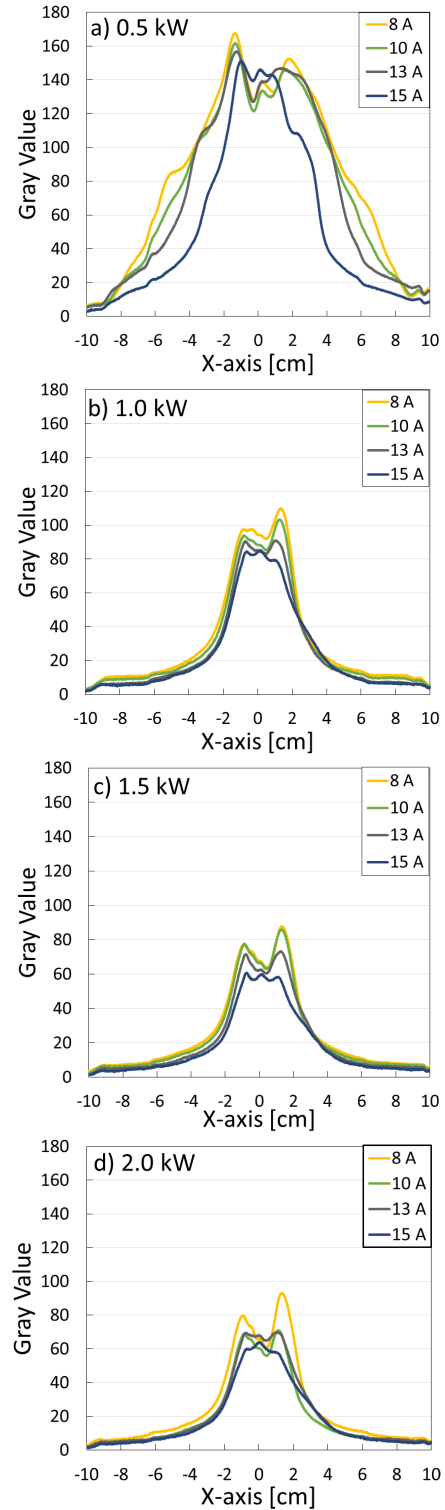

Fig. 5   (color online) Intensity of the plasma glow of the sheet plasma images at varying coil current for P_{mw} = a) 0.5 kW, b) 1.0 kW, c) 1.5 kW, d) 2 kW across the *x*-axis.

ness did not show significant reduction across the applied magnetic field.

3.2 T_e, n_e, V_{Plasma} and V_F
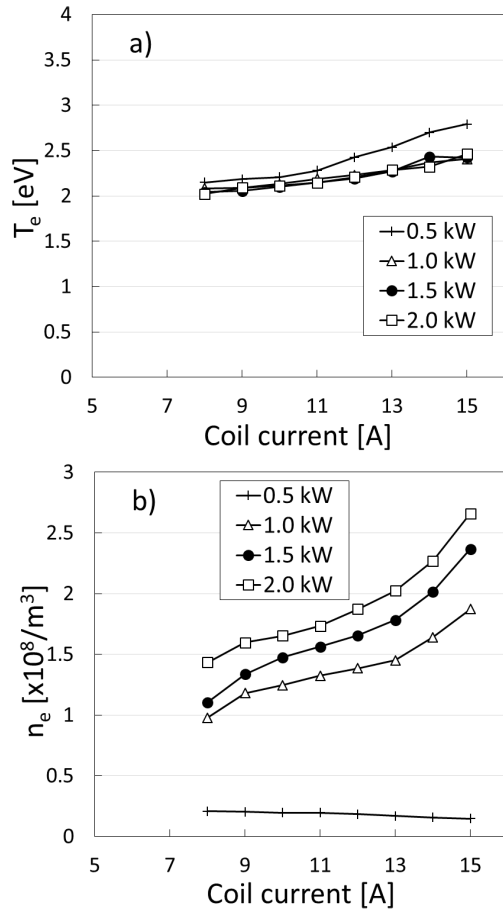
The measured probe *I-V* traces taken at the center of

Fig. 6 Plot of magnetic field (B) and microwave input power (P_{mw}) dependence of a) electron temperature (T_e), b) electron density (n_e).

Fig. 7 Plot of magnetic flux density (B) and microwave input power (P_{mw}) dependence of a) plasma potential (V_{plasma}), b) floating potential (V_F), and c) potential difference (V_{Plasma}-V_F) with corresponding electron temperature (V_{Plasma}-V_F)/$ln(M_i/2\pi m_e)$ calculation.

the plasma chamber ($x = 0$, $y = 0$) were analysed for T_e, n_e, V_{Plasma}, and V_F with respect to varying B and P_{mw} and are shown in Fig. 6 and Fig. 7. The probe location at the center of the chamber corresponds to the 17.5 cm distance from the quartz window surface. The overall behaviour of T_e, in Fig. 6 a), is largely dependent on the magnitude of the applied linear magnetic field. At a relatively low power of 0.5 kW, T_e is significantly higher than the higher input powers across the range of field intensities. For $P_{mw} \geq 1.0$ kW the measured T_e maintained the same range against increasing applied B and did not hint on the emergence of more energetic electron population due to the applied power in this region. The electrons at 0.5 kW appear to have higher energies than those excited at higher P_{mw}. Meanwhile, in Fig. 6 b), n_e increases towards higher magnetic flux density.

The plot of the plasma potential, V_{Plasma}, against the magnetic field intensity is shown in Fig. 7 a). A constant increase is observed as the current coil was increased while the floating potential, V_F, values plotted in Fig. 7 b) becomes more negative with increasing coil current. In accordance with the change in electron temperature that shows only a difference of 0.5 eV except for 0.5 kW case,
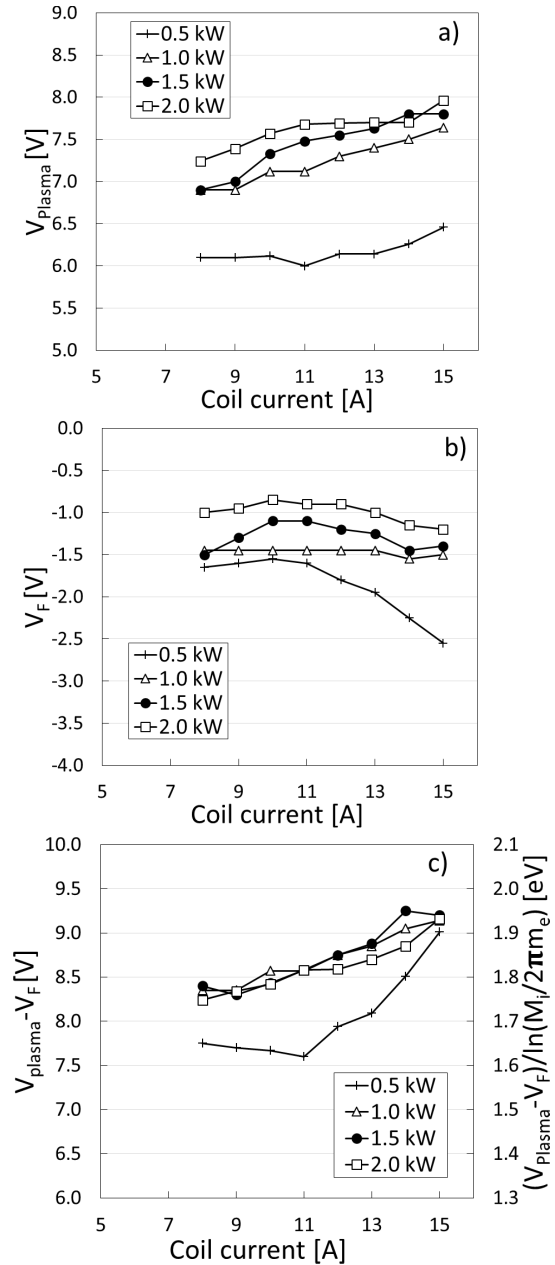
the potential difference (V_{Plasma}-V_F) did not change substantially larger than 1 eV, as derived from the function (V_{Plasma}-V_F)/ $ln(M_i/2\pi m_e)$ and shown in Fig. 7 c).

4. Discussion
4.1 Change in plasma parameters

From the results of plasma parameter measurements, one sees a marked difference between 0.5 kW data and those taken at higher input power. The comparison between 0.5 kW and 1.0 kW operation shows an order of magnitude jump in electron density. For higher power op-

eration, magnetic field intensity increased the electron density, while for 0.5 kW operation, n_e decreases gradually, though not significantly, against increasing B. This may correspond to a different plasma transport from the plasma excitation region to the chamber center.

The response of the plasma against the microwave power, showing a characteristic difference at 0.5 kW as described in Fig. 6, can be explained by the collision frequency between charged particles and neutrals which was observed in several [8–11]. A relatively higher T_e can arise from the lower electron different configuration density. A slight increase in the positive plasma potential hints an increase in local ionization rate supported by an increase in electron density while maintaining T_e. The derived floating potential, which is more negative at 0.5 kW, indicates the higher proportion of energetic electrons at 0.5 kW.

The effect of increasing the magnetic flux density can be clearly observed by the general increase in T_e, n_e (except 0.5 kW) and V_{Plasma} while V_F becomes more negative. The increase in T_e for higher magnetic flux density agrees with the findings in [1] and [3] who attribute the effect to Joule heating arising from the decrease in plasma current cross section leading to increase in energy yield per unit volume of plasma.

4.2 Effect of local gas injection

In the current plasma excitation configuration, a neutral gas flow intersects the plasma irradiation onto the quartz glass window (as depicted in Fig. 2). To see if this "local gas injection" affects the local plasma production near the microwave window, the luminous intensity distribution, L_i, of the produced plasma near the window was observed in the similar procedure to obtain the distribution shown in Fig. 4. The distribution in Fig. 4 was compared with the distribution, L_m, taken with the discharge gas supplied from the gas inlet 1 shown in Fig. 1. Expecting a cooling effect due to molecular activated recombination [12], hydrogen gas was introduced instead of Ar.

First, the luminous intensity distribution (L_i) profile of the plasma at varying pressure was obtained for the case of local hydrogen gas injection in the quart window. The luminous intensity distribution profile (L_m) for the case of gas injected at the main chamber center, away from the quartz window, was also obtained and compared with that of the latter. The derived intensity profiles are similar to those shown in Fig. 5. From here, the intensity profile comparison, (L_i - L_m), the difference in the obtained gray values, was derived and is shown in Fig. 8. The plasma profiles appear to be almost similar at 4 Pa. The effect of the local gas injection can be seen as an increase in the luminous intensity of the plasma and becomes more pronounced at higher pressure, or higher flow rate. The optical emission , however, showed no indication of substantial change in the wavelength spectrum due to excited molecules.
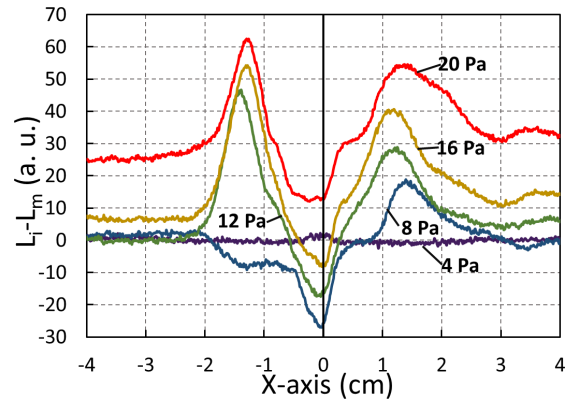

Fig. 8 (color online) Difference in the luminosity intensities between local gas injection and gas introduced mainly into the main chamber (L_i - L_m).

5. Conclusion

The effect of increasing the magnetic flux density in the microwave window region of a sheet plasma device with localized ECR was investigated. The electron temperature, electron density and plasma potential at the center increased at higher magnetic field, indicating better transport of plasma from the microwave excitation region. The plasma potential and the floating potential seem to suggest the presence of some high energy tail in the electron energy distribution function. Luminous intensity distributions of the plasma glow show a clear difference between two different ways to supply discharge gas: local injection at the microwave window and at the central region of the plasma chamber. The local injection changes the spatial distribution of the plasma optical glow due to neutral gas flow, and the effectiveness of the flow for window cooling has to be confirmed in the future study.

[1] I.A. Krinberg, Tech. Phys. Lett. **29** (6), 504 (2003).

[2] E. Hashemi, K. Niayesh and H. Mohseni, Turk. J. Elec. & Comp. Sci. **24**, 4957 (2016).

[3] M. Galonska, R. Hollinger, I.A. Krinberg and P. Spaedtke, IEEE Trans. Plasma Sci. **33** (5), 1542 (2005).

[4] H.J. Woo, K.S. Chung, M.J. Lee and T. Lho, Phys. Plasmas **16**, 023505 (2009).

[5] M. Yoshida and K. Kajinishi, IEEE Trans. Plasma Sci. **31**, 40 (2003).

[6] A.R.B. Gines and M. Wada, Plasma Fusion Res. **14**, 3401085 (2019).

[7] O. Tarvainen *et al.*, Plasma Sources Sci. Technol. **23**, 025020 (2014).

[8] A.T.T. Mostako *et al.*, IEEE Trans. Plasma Sci. **44** (1), 7 (2016).

[9] S.F. Yoon *et al.*, Vacuum **61**, 29 (2001).

[10] C.A. Outten, J.C. Barbour and W.R. Wampler, J. Vac. Sci. Technol. A **9** (3), 717 (1991).

[11] C. Moon, S. Tamura, T. Kaneko and R. Hakakeyama, J. Plasma Fusion Res. **9**, 436 (2010).

[12] N. Ohno, N. Ezumi, S. Takamura, S.I. Krasheninnikov and A.Y. Pigarov, Phys. Rev. Lett. **81**, 818 (1998).